International Journal for Innovative Engineering and Management Research
A Peer Revieved Open Access International Journal
www.ijiemr.org

COPY RIGHT

IJIEMR Transactions, online available on 25th Apr 2020. Link
:http://www.ijiemr.org/downloads.php?vol=Volume-09&issue=ISSUE-04

Title: CONTROL OF HYBRID BOOST CONVERTER FOR A PV CHARGING STATION USING PARTICLE SWARM OPTIMIZATION TECHNIQUE

Volume 09, Issue 04, Pages: 87-101
Paper Authors

KAVALI BABITHA, DR.G.S.DURGA PRASAD

International Journal for Innovative Engineering and Management Research
A Peer Revieved Open Access International Journal
www.ijiemr.org

CONTROL OF HYBRID BOOST CONVERTER FOR A PV CHARGING STATION USING PARTICLE SWARM OPTIMIZATION TECHNIQUE

[1]KAVALI BABITHA,[2]DR.G.S.DURGA PRASAD
[1]PG Student,[2]Professor
[1,2] Department of Electrical and ElectronicEngineering, J.B.Institute of Engineering and Technology, Hyderabad.
ksonymudiraj@gmail.com

Abstract: Hybrid Boost Converter (HBC) is proposed to supplant DC/DC converter just as DC/AC converter in request to diminish switching misfortunes and distinctive change stages. In this paper, the framework contains a PV framework, a HBC, Plug-in Hybrid Electric Vehicle (PHEV) and AC framework. The Particle Swarm Optimization (PSO)–MPPT calculation is intended to separate most extreme power from the PV array. MPPT , PLL and Vector control plans are utilized to control the exhibition of HBC. It is utilized to follow Maximum Power (MPPT),realize DC voltage regulation ,receptive power control and power management. A testbed using power hardware switching devices is structured in MATLAB/SimPowersystems for approval. Reproduction results represent the attainability of structured control design.

Index Terms – Hybird Boost Converter (HBC) , Plug-in Hybrid Electric Vehicle (PHEV) , Photovoltaic (PV) , Maximum Power Point Tracking (MPPT), Particle Swarm optimization(PSO).

I. INTRODUCTION

There might be increment in number of creation and utilization because of monetary and ecological preferences of PHEV [2]. The U.S. Division of Energy exhibited that more than one million PHEVs will get sold in the U.S. by one decade from now [3]. Research was directed on building up a charging station by interfacing a three-stage air conditioning lattice with PHEVs [4]–[6]. The distinctive PHEV charging topologies and strategies are looked at and assessed in [2], [7]. In any case, a huge scope entrance of PHEVs may expand pressure on the matrix during charging periods.Hence, accusing stations of PV as an extra force source has become a crucial arrangement.

For PV charging stations, a design and controllers is proposed in [8]. By considering the matrix's stacking limit the charging the executives is created in [9]. For this kind of frameworks, controlling at any rate three diverse force electronic converters to charge PHEVs is fundamental. Every converter needs an individual controller, that thus expands multifaceted nature and system power losses. Successively, to lessen the quantity of changing over stages it is earnest to research multiport converters.

The goal of this paper is to execute a multi-port converter for PHEVs in a PV charging station and structure a controller for it.

II. THREE-PHASE HBC-INTERFACED PV CHARGING STATION OPERATION AND TOPOLOGY

A three-stage HBC uses indistinguishable number of changes same from two-level voltage source converter (VSC). The HBC acknowledges both dc/dc just as dc/air conditioning transformation. For examination, Fig.2.1 outlines the PV charging station where a dc/dc help converter and

International Journal for Innovative Engineering and Management Research
A Peer Revieved Open Access International Journal
www.ijiemr.org

a three-stage VSC are utilized to interface the PV framework, the air conditioner matrix and PHEV's. Fig.2.2 shows the HBC-interfaced PV charging station's topology. The primary parts of the PV charging station comprise of PV cluster, three-stage bidirectional HBC, PHEV's batteries, air conditioning network and off-board dc/dc converter.

Comprehension of three-stage HBC activity is important to plan a controller. HBC activity is accessible in detail in[11], [12], [17].

The PV side comprises of a huge inductance to accomplish ceaseless condition and capacitance is to diminish the voltage swell sign. The dc side comprises of a diode, a dc transport for associating PHEV, a dc capacitor to dispense with the waves in yield current, an off-board unidirectional confined dc/dc converter and batteries of PHEV's. The acsystem contains , a step up transformer, a three-phase LC channel, and the point of common coupling (PCC) transport to associate the PV station to the fundamental grid.

The PV array is a mix of interfacing series cells and parallel strings. Contingent upon the sort and planning criteria each PV cell has explicit qualities. PV models essentially rely upon Shockley diode condition [18], [19]. PV is structured as photon-produced current source utilizing an equal two-diode framework and a shunt resistor, Rsh, just as an arrangement resistor, Rs[18] contains numerical conditions for two-diode cell of PV. A solitary IGBT-VSC has the capacity to work in high voltage rating subsequently, HBC-interfaced PV charging station has ability to work in medium just as high power ratings of PV power plants.

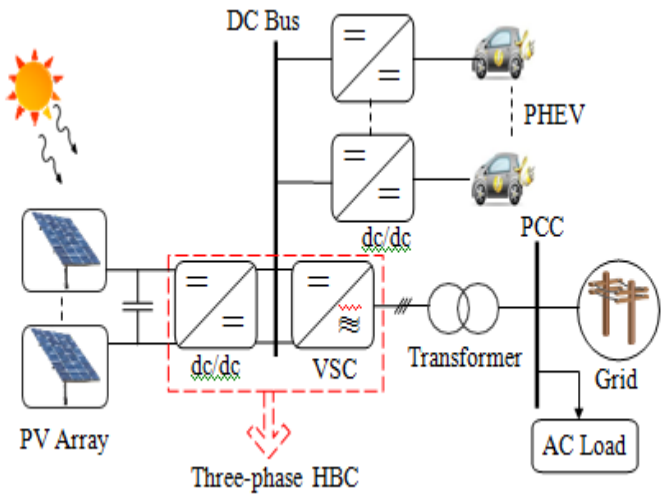

Figure 2.1 PV charging stationArchitecture configurations.

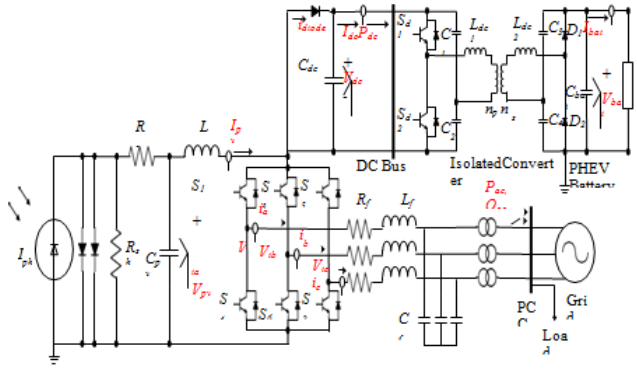

Figure 2.2 Three-phase HBC-interfaced PV charging

Dc/dc converter has two operating modes which are “on” and “off”. Whereas VSC has “active” and “zero” operating modes. Here, three-phase HBC integrates operating modes of both dc/dc converter and VSC into three main operating modes as: shoot-through (ST) mode, zero mode (Z) and active mode (A).

Steady-state operation of three-phase HBC is better illustrated by considering following assumptions,First, system is assumed as lossless. Second, as voltage drop on each diode is very small so it is ignored. Third, HBC is operated in inverter mode when power flows from PV to grid. It is observed that HBC can be operated in converter or inverter mode based on power flow

International Journal for Innovative Engineering and Management Research
A Peer Revieved Open Access International Journal
www.ijiemr.org

direction. Lastly, during the active phase the diode current is continuous. Below given are the steady-state relations between PV, ac side and dc side

$$Vdc = \frac{Vpv}{1-Dst}\ , Vac = Mi\frac{Vdc}{2} (2.1)$$

$$VLL = Mi\frac{\sqrt{3}Vdc}{2\sqrt{2}} = 0.612\frac{Mi}{1-Dst}Vpv \qquad (2.2)$$

where M_i= the ac voltage per-phase modulation index,

D_{st}= duty cycle of the shoot-through period,

Vdc = the peak dc voltage,

Vac = peak per-phase ac voltage,

V_{LL} = theRMSvalueoftheline-to-lineoutputacvoltage.

It is concluded from equation (2.2) that dc output depends on only $D_{st}$and ac output depends on both $M_i$and D_{st}. The controlling signs need to accomplish this condition to accomplish consistent control of changed PWM:

$$M_i + D_{st} < 1 (2.3)$$

2.1 MODIFIED PWM

To handle the switching states of a three-phase HBC sinusoidal PWM and dc PWM are not appropriate. Instead of controlling ac and dc outputs separately using HBC switches, a modified PWM is used to manage two outputs at the same time. During shoot-through period, one leg of HBC turns on. At this mode PV side current streams into switches of single leg. Inductor gets charged at this mode. During zero mode, all the upper switches are on while lower switches are off. PV side current all streams to the dc side that is battery frameworks at this mode.Finally, during active mode all the current flows into the ac system.

Five signalsarethree-phaseacsignalsV_a,V_b,V_c,dcsignalsV_{st} and $-V_{st}$ which are controlled by modified PWM to regulate the switching states. Modified PWM controls both dc and ac outputs at the same time. This is the main advantage of using modified PWM.

III.CONTROL OF PV CHARGINGSTATION

This section provides detailed view about the controller of three-phase HBC-interfaced PV charging station. From equation(2.2), HBC uses D_{st} to boost PV voltage and modulation index M_i to regulate ac voltage magnitude. To achieve active and reactive power regulation, angle of three-phase ac voltage V_t can be adjusted. At the point when ac system is even and adjusted, complete three-phase instantaneous power is consistent and consequently the average power of ac approaches the net power at dc side (P_{ac} = $P_{pv}P_{dc}$).

The controller consists of three main blocks: MPPT, Phase-locked loop (PLL) and the vector control as shown in Fig.3.1.

$S_1 - S_6$

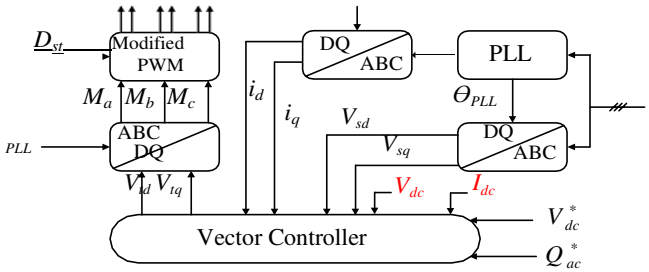

Figure 3.1 Control blocks of HBC-interfaced PV charging station.

3.1PSO -MPPT

A basic PSO algorithm works by having a population (called a swarm) of candidate solutions (called particles). These particles move around the search-space according to few simple formulae called fitness function. The movement of particles are guided by their own best known position in the search-space and the whole best known position of swarm. When improved

positions are discovered particles will then come to guide the movements of the swarm. The process is repeated and the iterations stop when similar values of fitness function are obtained.

Particle swarm optimization (PSO) calculation is a stochastic optimization method dependent on swarm, which was proposed by Eberhart and Kennedy (1995) and Kennedy and Eberhart(1995). PSO calculation reenacts creature's social conduct, including creepy crawlies, crowds, winged animals and fishes. These swarms affirm a helpful method to find nourishment, and every part in the swarms continues changing the hunt design as indicated by the learning encounters of its own and different individuals. PSO additionally utilizes a swarm mode which makes it to at the same time search huge locale in the arrangement space of the advanced target work. In examining the conduct of social creatures with the artificial life hypothesis, for how to build the swarm artificial life frameworks with helpful conduct by PC, Million has proposed five essential standards:

(1)**Proximity:** the swarm ought to have the option to do basic reality calculations.
(2)**Quality:** the swarm ought to have the option to detect the quality change in the earth and response it.
(3)**Diverse response:** the swarm ought not restrict its approach to get the assets in a limited degree.
(4)**Stability:** the swarm ought not change its conduct mode with each natural change.
(5)**Adaptability:** the swarm should change its conduct mode when this change is commendable.
These five standards have become core values for the swarm artificial life framework. In PSO, particles can refresh their velocities and positions as indicated by condition changes.
The swarm in PSO won't limit its development yet persistently look through the optimal arrangement in the conceivable arrangement space. Particles in PSO keeps their steady development in the hunt space, while change their development to adjust the adjustment in nature. Consequently, particle swarm framework meets the above five standards.

3.1.1 The motivation behind PSO :

The typical point of the particle swarm optimization (PSO) algorithm is to tackle an unconstrained minimization issue: discover x* with the end goal that f(x*)<=f(x) for all d-dimensional genuine vectors x. The objective function f: Rd >= R is known as the fitness function.

3.1.2 Swarm topology

Every particle i has its local Ni (a subset of P). The structure of the areas is known as the swarm topology, which can be spoken to by a chart.
Attributes of particle i at cycle t:

- xi (t): the position of the particle
- pi (t): the "historically" best position
- li (t): the historically best position of the neighbor particles
- vi(t): the speed; it is the size of venture between xi (t) and xi (t+1)

The particle positions are introduced arbitrarily toward the start of the algorithm and the velocities are set to 0, or to some little arbitrary qualities.
Parameters of the algorithm:

- w(t): inertia weight; a damping factor, generally diminishing from around 0.9 to around 0.4 during the calculation.
- φ1, φ2: speeding up coefficients; ordinarily somewhere in the range of 0 and 4.

3.1.3Speed and positions of the particles

The particles update their speed using the the formula,

$$Vi^{t+1} = W^{t}Vi^{t} + \emptyset 1u1(Pi^{t} - Xi^{t}) + \emptyset 2u2(Ii^{t} - Xi^{t}) \quad (3.1)$$

The symbols u_1 and u_2 represent random variables with the U(0,1) distribution. The first

International Journal for Innovative Engineering and Management Research
A Peer Revieved Open Access International Journal
www.ijiemr.org

part of the velocity formula is called "inertia", the second part is called "the cognitive (personal) component", the third part is called "the social (neighborhood) component". Position of particle i changes according to

$$Xi^{t+1} = Xi^{t} + Vi^{t+1} \quad (3.2)$$

3.1.4 Stopping rule

The algorithm is terminated after a given number of iterations, or once the fitness values of the are close enough.

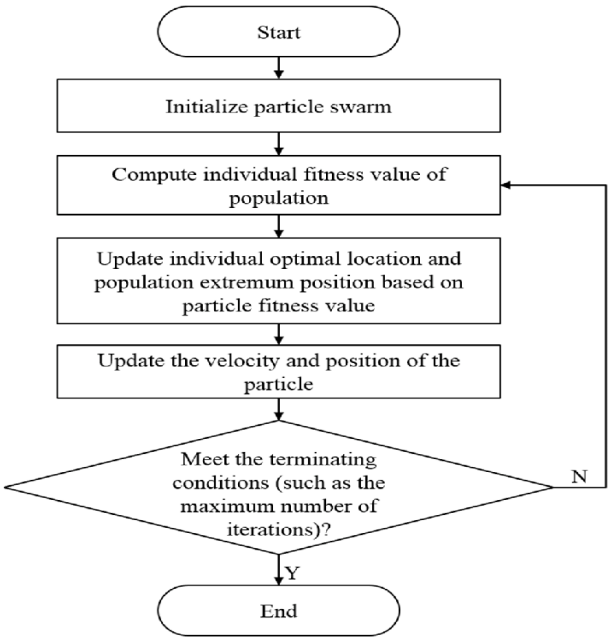

Figure 3.2 PSO Algorithm Flow chart

3.2SYNCHRONOUS ROTATING FRAME-BASED PHASE-LOCKED LOOP(SRF-PLL)

As the PV charging station requires ac grid as a backup supply, three-phase HBC is worked at grid tied mode. Incorporation of the three-phase HBC needs to fulfill IEEE-1547 standard which requires synchrony of the phase and angular frequency of the three-phase HBC with the fundamental network [24], [25]. Synchronous rotating frame-based phase-locked loop (SRF-PLL) adjusts the space vector of the point of common coupling (PCC) voltage to the d-axis and powers the q-axis PCC voltage Vsq to zero utilizing a PI compensator as appeared in Fig.3.3.

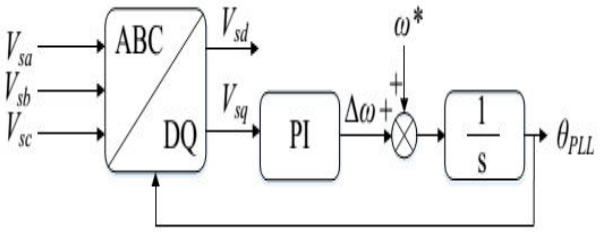

Figure 3.3 Basic schematic diagram of a SRF-PLL

$$Gpll = \frac{Kp,pll+Ki,pllS}{S}\frac{Vsd}{S} \quad (3.3)$$

where $K_{p,PLL}$, $K_{i,PLL}$ = compensator parameters

Vs = grid's voltage amplitude.

With an oscillation mode with a damping factor ζ and a natural frequency ω_n, the closed-loop transfer function of SRF-PLL is a second-order system. The parameters of the compensator are selected as:

$\zeta = 1/\sqrt{2}$; ω_n= the reference frequency of the grid ω. The resulting parameters are:

$$Ki, pll = \frac{\omega^2}{Vs}, Kp, pll = \frac{2\zeta\sqrt{Ki,pll}}{Vs} \quad (3.4)$$

3.3VECTOR CONTROL

VSC requires vector control technique. The ac current is controlled by the inner loop while the dc voltage and reactive power are controlled by the outer loop. Consideration of D_{st} is the main difference of HBC.

The response of inner is designed to respond faster than outer loop to reject disturbances and for fast response. The response of inner loop is in milliseconds and that of outer loop is 10 times slower to achieve fast transient response. The open-loop of the inner current loop consists of the PI compensator, the transfer function of the plant, the delay of the modified PWM.

$$Gi, ol(s) = \left(Kpi + \frac{Kii}{s}\right)\frac{1}{Lfs+Rf}\frac{1}{TpwmS+1} \quad (3.5)$$

where T_{PWM} = time delay of switching frequency

International Journal for Innovative Engineering and Management Research
A Peer Revieved Open Access International Journal
www.ijiemr.org

of the modified PWM;

K_{pi} and K_{pi} = the PI compensator's parameters for the inner current loop;

L_f and R_f are the inductance and resistance filter components of the converter.

The RL circuit dynamics dominates the pole which is cancelled by the zero of the PI controller. The open-loop transfer function becomes

$$\text{Giol(s)} = \frac{1}{\text{STpwm(TpwmS+1)}} \qquad (3.6)$$

by choosing the following parameters:

$$\text{Kpi} = \frac{\text{Lf}}{\text{Tpwm}}, \text{K}_{\text{ii}} = \frac{\text{Rf}}{\text{Tpwm}}.$$

Other advantage of HBC-interfaced PV station is it generates a supported reactive power for grid. The delivered reactive power of the HBC at PCC is calculated as:

$$\text{Qpcc} = \frac{-3}{2}\text{Vsdi} \qquad (3.7)$$

where V_{sd} = the projection of the ac voltage component on d axis of the stationary reference frame;

i_q = the projection of the output current of HBC on q reference frame.

The open loop transfer function of the reactive power controller is given as :

$$\text{Gol(s)} = \text{GQ(s)Gpi(s)Gsw(s)Gi(s)}$$

$$\text{Gol(s)} = \left(\frac{3}{2}\text{Vsd}\right)\left(\frac{\text{kpQS+kiQ}}{\text{S}}\right)\left(\frac{1}{\text{TpwmS+1}}\right)\left(\frac{1}{\text{LfS+Rf}}\right) \qquad (3.8)$$

where k_{pQ} and k_{iQ} are the PI compensator's parameters. The open-loop and closed loop transfer functions of the reactive power equation are driven using modulus optimum technique on Equation (3.8) as:

$$\text{Gol(s)} = \frac{1}{\tau\text{Qs(TpwmS} + 1)}$$

$$\text{Gcl(s)} = \frac{1}{\text{Tpwm}\tau\text{Qs}^2 + \tau\text{Qs} + 1}$$

$$\text{kp} = \frac{3}{2}\frac{\text{VsdLf}}{\tau\text{Q}}\ ;\ \text{ki} = \frac{3}{2}\frac{\text{VsdRf}}{\tau\text{Q}} \qquad (3.9)$$

where τQ = the time constant of the resultant closed-loop system.

Equation (3.9) represents a general form of the second order system. Equation (3.8) is used for frequency of natural oscillation as $\omega n = \sqrt{\frac{1}{\text{Tpwm}\tau\text{Q}}}$ while the damping factor as $\zeta = \sqrt{\frac{\tau\text{Q}}{4\text{Tpwm}}}$.

Accepting there is no switching power loss, the steady-state operation of power balance relationship of the three-phase HBC is given as:

$$\text{Ppv} = \text{Pcap} + \text{Pdc} + \text{Pac} \qquad (3.10)$$

$$\text{Pac} = \frac{3}{2}\text{Vsdid} \qquad (3.11)$$

where i_d and V_{sd} are the projections of the ac current and grid voltage space vectors on the d-axis. The power relationship is further expressed as follows.

$$\text{Pcap} = \text{CVdc} = \text{Ppv} - \text{Pac} - \text{Pdc}$$

$$= \text{VdcIpv} - \frac{3}{2}\text{Vsdid} - \text{VdcIdc}$$

Therefore, the dynamics of the capacitor voltage can be expressed as follows.

$$\text{C}\frac{\text{dVdc}}{\text{dt}} = \text{Ipv} - \frac{3}{2}\frac{\text{Vsd}}{\text{Vdc}}\text{id} - \text{Idc} = \text{ud} \qquad (3.12)$$

The dc voltage error $V_{dc}^* - V_{dc}$ is reduced by negative feedback controller and PI controller amplifies it. Ud is the output of PI controller. The reference signal i^*_d is generated from this signal as:

$$\text{Id} * = \frac{2}{3}\frac{\text{Vdc}}{\text{Vsd}}(\text{ud} - \text{Ipv} + \text{Idc})$$

The open-loop transfer function of outer voltage is given as:

$$\text{Gv, ol(s)} = \left(\text{Kpv} + \frac{\text{Kiv}}{\text{s}}\right)\frac{1}{\tau\text{is}+1}\frac{1}{\text{Cs}} \qquad (3.13)$$

International Journal for Innovative Engineering and Management Research
A Peer Revieved Open Access International Journal
www.ijiemr.org

where τ_i = the time constant for the inner current closed loop.

Two poles at origin are included by the open-loop transfer function for voltage controller.

Double integrators are dealt using a technique called Symmetrical optimum [27]. The concept involved is to slow down the dynamic response and increase phase margin symmetrical optimum operates at a low frequency. The compensator parameters are given based on the symmetrical optimum method as follows:

$$Tiv = a^2 2\,\tau i\,, Kpv = \frac{C}{K\sqrt{Tiv}\sqrt{\tau i}}, Kiv = \frac{Kpv}{Tiv} (3.14)$$

where K = 3Vsd/2Vdc

a = the symmetrical frequency range between peak phase margin and low frequency operation area.

To achieve high phase magin it is very necessary to select a high value of the symmetrical gain a. The value of a lies between 2 and 4 [28].

3.4 CONTROL OF OFF-BOARD BATTERY CHARGER

Lithium-ion batteries are mostly used by PHEV manufacturers to operate vehicles like Chevy Volt and Nissan Leaf. An identical electrical battery cell model is appeared in Fig.3.5. battery comprises of a capacitor C and a current-controlled current source to speak to the life of battery.Transient and steady state thevenin-based model and voltage-controlled open circuit voltage source which depends on state of charge (SOC)in battery cells or the amount of available energy are alo included.

A total model of PHEV battery is used at the present time. Fig.3.6 speaks to the equivalent circuit of interfacing PHEV batteries that are related with the PV charging station. Course of action relationship of battery cells increase the voltage and equivalent grows the full scale energy. Each PHEV's battery contains M branches and each branch contains N-cells. The absolute model is showed up in Fig.5.8. The detaild parameters of the business PHEV are given in [29].

The different types of PHEV battery charging schemes are:constant current (CC), constant voltage (CV), and taper-current (TC) [32]–[34]. CV is implemented through vector control of HBC, which regulates the dc-link voltage.

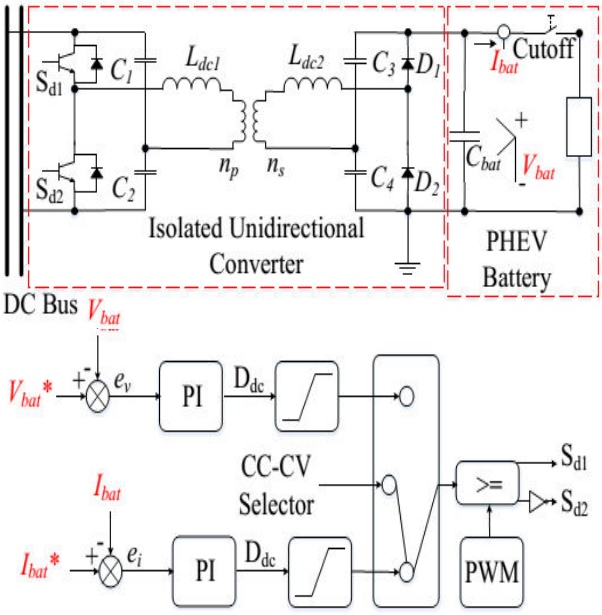

Figure 3.5 off-board charging structuresingle battery cell circuit model using CC-CV algorithm

International Journal for Innovative Engineering and Management Research
A Peer Revieved Open Access International Journal
www.ijiemr.org

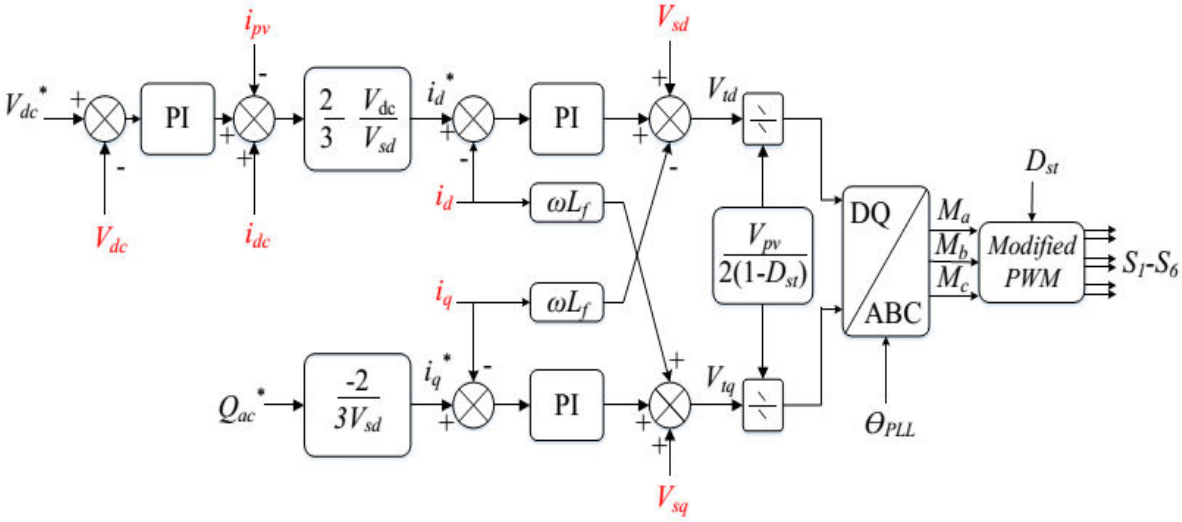

Figure 3.4 Three-phase HBC Vector control scheme

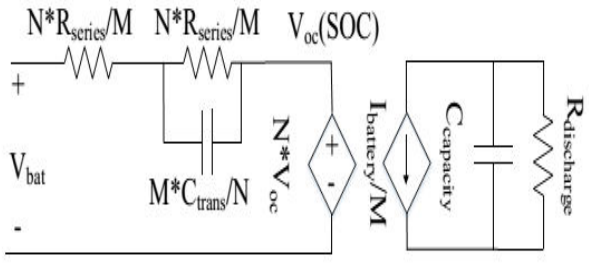

Figure 3.6 PHEV Li-ion battery module Equivalent circuit

CV and CC both are used to realize optimal charging scheme which is adopted through off-board unidirectional isolated dc/dc converter. Here, it is adopted to increase the life cycle and performance of battery and to minimize damage to PHEV's batteries due to fast charging.

To protect battery from PV power source and grid terminal, the PHEV's battery is isolated. Fully galvanic isolation of PHEV's battery is provided by the charging station towards main distribution network PV station dc bus. Isolated off-board is essential for safety considerations since isolated on-board chargers are not used because of weight and cost.

During charging period, PHEV's battery is confined from rest of the framework by utilizing a high-recurrence transformer on the off-board converter. More wellbeing of PHEV's battery and better change of voltage are favorable circumstances of utilizing this topology. A separated unidirectional half-bridge converter as appeared in Fig.3.5 is being remembered for the setup of off-board charging converter.

Charging control is deliberately intended for quick charging of PV stations particularly since a battery stockpiling framework is the more costly and progressively disparaging of PHEV. Battery can prompt unnecessary harm because of increment in temperature, in the event that it spans to full charge and high charging current is proceeded or toward the start of the procedure charging by utilizing quick charging strategy [32].So consideration of above mentioned consequences is necessary in designing a control for PV charging stations.

CC charging method charges relatively with uniform current. It does not consider the battery state of charge(SOC). It mainly depends on low or high constant charging current. These help in eliminating the imbalances between cells and intensify the battery's life cycle. Although, high

International Journal for Innovative Engineering and Management Research
A Peer Revieved Open Access International Journal
www.ijiemr.org

charging current results in excessive damage while low charging current is not suitable to charge the battery faster.

CV charging method does not depend on the state of charging (SOC) of battery. The input voltage is limited to a specified level. Due to high potential difference between the charger and the battery it results in high initial current. So in order to avoid such high initial current the knowledge of battery's initial voltage is required. As PHEVs exists with different battery characteristics the above requirement is difficult to satisfy in real applications.

The TC charging method proportionally decreases charging current with rise in battery's voltage. Prevention of overheating issues and gasification is the main advantage of this method. But due to different PHEV's battery characteristics enforcement of this method is difficult in real time applications is tough.

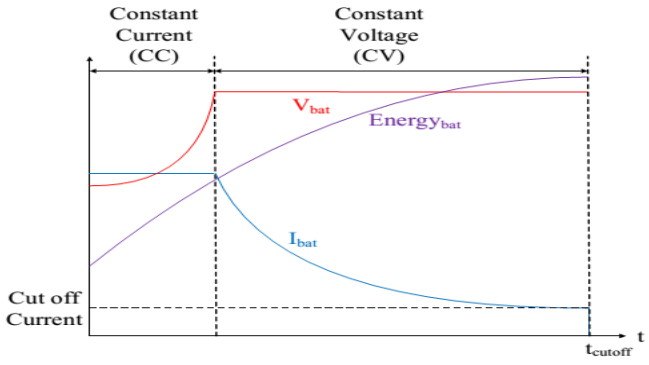

Figure 3.7 PHEV's battery charging using CC-CV technique

For efficient and reliable operation of PV charging station and considering above mentioned features of all the three methods here CC and CV methods are integrated and introduced. It is implemented in a dc/dc converter as shown in Fig.3.7.

First constant current method charges the battery so as to avoid initial high current in CV method. Then to keep away from overcharge the control is switched to CV method as soon as voltage of battery goes to rated value. At last, when battery's current achieves cut-off line and energy achieves full charged region, the PHEV is disconnected using controller for protection. Thus, the advantages of applying CC-CV method is to protect PV charging station from overheat and overcharge.

The battery's measured components are regulated using two control loops as shown in Fig.3.5. the off-board dc/dc buck converter and PHEV battery detailed configuration is also shown. To prefer an operational mode for charger so that it disconnects battery as soon as it gets fully charged is the main goal of the selector.

Table 4.1 system parameters

	PARAMETER		**PARAMETER**
PV	V_{oc} =65.1V V_{mpp} =54.7V I_{sc} =6.46A I_{mpp} =5.98A R_{sh} =298.531Ω R_s =0.369Ω	AC	$V_{grid\ (L-L)}$ = 20Kv ω = 377rad/s S =100kVA $V_{t(L-L)}$ =208V R_f =2mΩ L_f =125μH C_f =150μF
DC	V_{dc} =350V L =5mH Load =100kV L_{dc} =10mH C_{dc}	Control	K_{pi} =0.625Ω K_{ii} =10Ω/s K_{pv} =0.24$Ω^{-1}$ K_{iv} =300$Ω^{-1}$/s

International Journal for Innovative Engineering and Management Research
A Peer Revieved Open Access International Journal
www.ijiemr.org

	=100μF		K_{pvdc} =0.001 K_{ivdc} =25 K_{iidc} =0.001 K_{iidc} =3
Chevy	# of cells:200 V_{cell} =1.25V Q_{energy}=16kWh Type :Li-Ion	Nissan	# of cells:160 V_{cell} =1.875V Q_{energy} =24kWh Type :Li-Ion

The proposed system is tested to check CC-CV method of charging conduction. CC method first charges with fast dc of 40A and charges upto 360V which is the rated voltage of battery of Chevy Volt vehicle. It is reached at 1.5 seconds. Later CV method of control operates decreasing battery current to cut-off region moderately. The same process is performed for all the vehiclesof PV charging station.

IV. SIMULATIONRESULTS

Three-phase HBC is implemented in PV charging station using the proposed control and case studies are performed in MATLAB/SimPowerSystems. Sunpower SPR-E20-327 is the PV model used in this paper.The required PV data and parameters of the system are as shown in Table I.

PHEV batteries are represented using the parameters of Nissan Leaf and Chevrolet Volt batteries [7], [35], [37]. Six case studies are performed to illustrate MPPT, voltage regulation, reactive power control and power management of the designed PV charging station.

4.1CASE 1: PERFORMANCE OF THE PSO - MPPT

The PSO-MPPT algorithm is executed in this case study. Fig.4.1 shows the implementation of MPPT due to change in solar irradiance.

The duty cycle D_{st} is generated from the MPPT that relates dc voltage V_{dc} and voltage of PV V_{pv} . Vector control is responsible to maintain dc voltage V_{dc} at 350V meanwhile supplying the reactive power Q*acto ac grid. Adjusting duty cycle and output voltage of PV to extract maximum power is the main role of MPPT as shown in Fig.4.1.

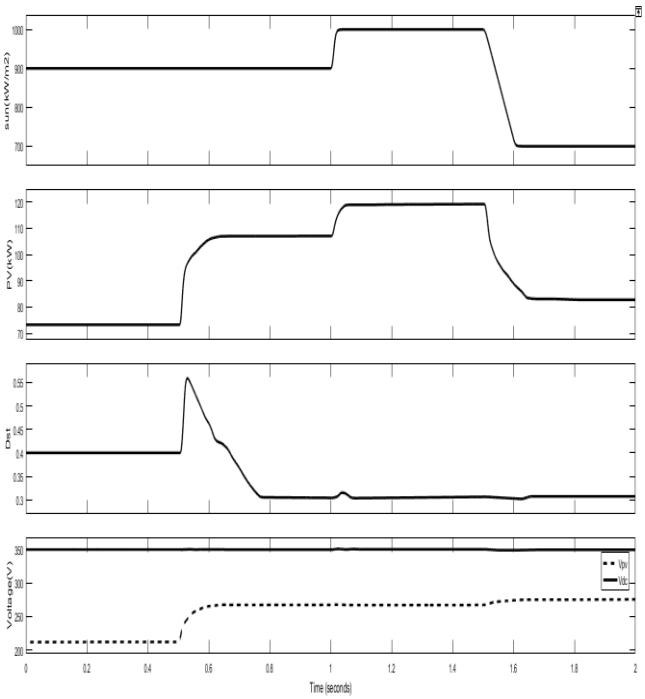

Figure 4.1 Performance of PSO-MPPT when sun irradiance changes

From 0-0.5 seconds, MPPT is not activated and the radiation of sun is 0.9 kW/m^2. At t=0.5 seconds, MPPT is activated. So the PV power increases from 70kW to 105kW. The duty cycle reduces and voltage of PV is picked up. V_{dc} has no effect of MPPT turning on and off.

Even if sun irradiation changes at t=1 and t=1.5 seconds the PV power attains higher value rather than decreasing. This shows the best performance of MPPT and results also validates this point.

International Journal for Innovative Engineering and Management Research
A Peer Revieved Open Access International Journal
www.ijiemr.org

4.2 CASE 2: PV CHARGING STATION POWER MANAGEMENT

To charge the PHEVs when there is not sufficient power at the PV side is the main aim of this case study.The dc load takes 50 kWh that shows charging of two Nissan Leaf vehicles supplying remaining power to the ac grid. When PV power decreases due to change in the sun radiation at t=0.5 seconds. As two more vehicles are added at t=1 and t=1.5 seconds it is observed that PV supplies power to third vehicle also.

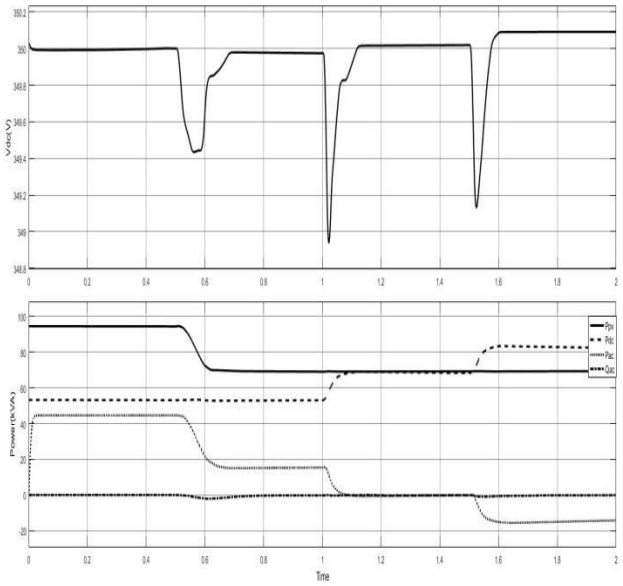

Figure 4.2 PV charging station Power management

Fourth vehicle is added at t=1.5 seconds. As the three-phase HBC operates in both the directions the controller allows load to absorb dc power from the ac grid. It also maintains constant dc voltage of 350V. The duty cycle ratio D_{st} and the modulation index M_i are shown in Fig.4.3.

4.3 CASE 3:DCVOLTAGECONTROLLER

As modified PWM controls ac and dc outputs at the same time three-phase HBC has the advantage of supplying dc and ac power at the same time.Whether MPPT control is on or off, the dc voltage is at 350V as dc voltage control is enabled. This implies that vector control in turn puts dc voltage constant as shown in Fig.4.4.

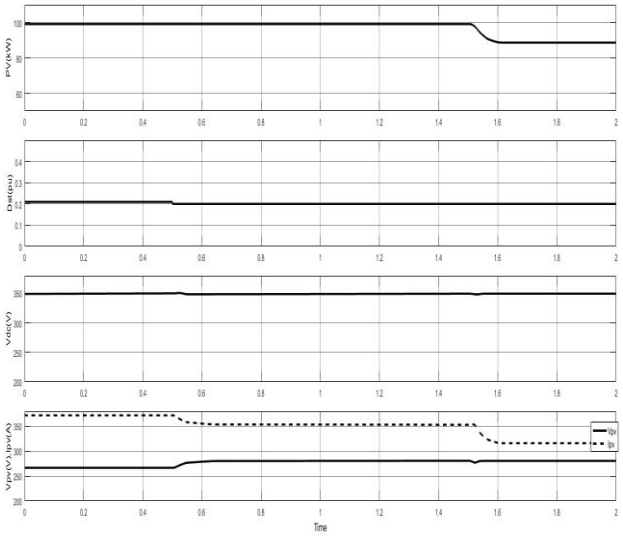

Figure 4.4 Dc voltage control in the vector control.

4.4 CASE 4: REACTIVE POWER CONTROL

The vector control of three-phase HBC plays a major role in controlling reactive power and real power. This is advantageous to track the performance of reactive power keeping dc voltage constant.

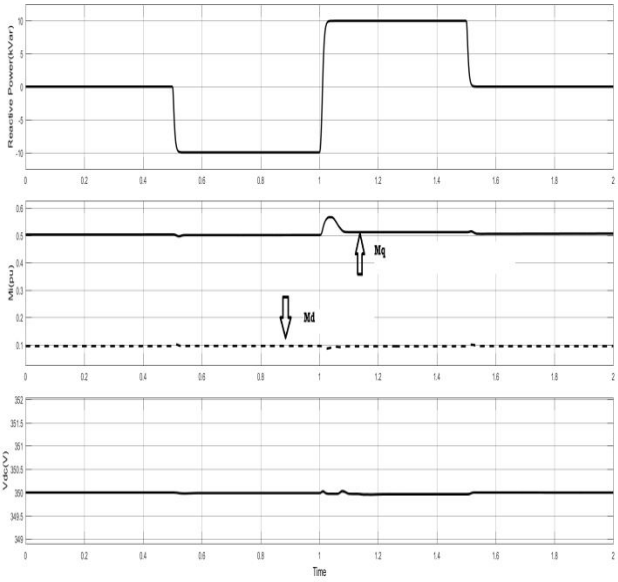

Figure 4.5 Proposed vector control to supply or absorb reactive power independently.

International Journal for Innovative Engineering and Management Research
A Peer Revieved Open Access International Journal
www.ijiemr.org

The reference reactive power first absorbs 10 kVAr at t=0.5 seconds and supplies 20kVAr to ac grid at t=1 seconds. The results confirm that the controller is designed in the best way to control reactive power and regulate dc voltage at 350V

4.5 CASE 5: PARTIAL GRIDFAILURE

Usually when a transmission line is subjected to a voltage sag of below 80% , the PHEVs need to be disconnected from grid [37]. The goal of the designed controller is to charge the vehicles continuously and constantly irrespective of any fault on the main grid.

Firstly the charging station and grid are connected to charge PHEVs. At t=0.5 seconds MPPT is turned on. At t=1 seconds a symmetrical voltage sag of 70% is encountered. The proposed control scheme settles this issue as seen in Fig.4.6.

Until the occurrence of failure all the power values are constant. The grid failure occurs between t=1 and t=1.5 seconds. At this stage, load power decreases from 20kW to 10kW. Even so the grid power rises from 20kW to 30kW.

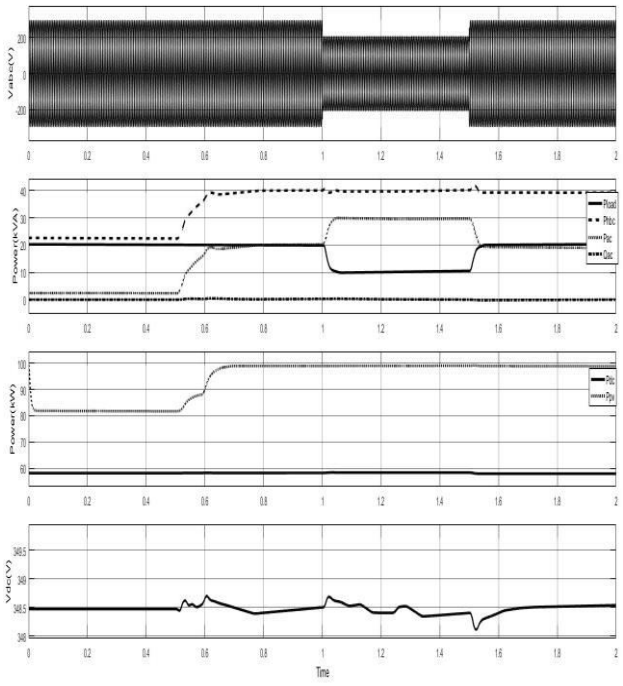

Figure 4.6 Under 70% grid's voltage drop.

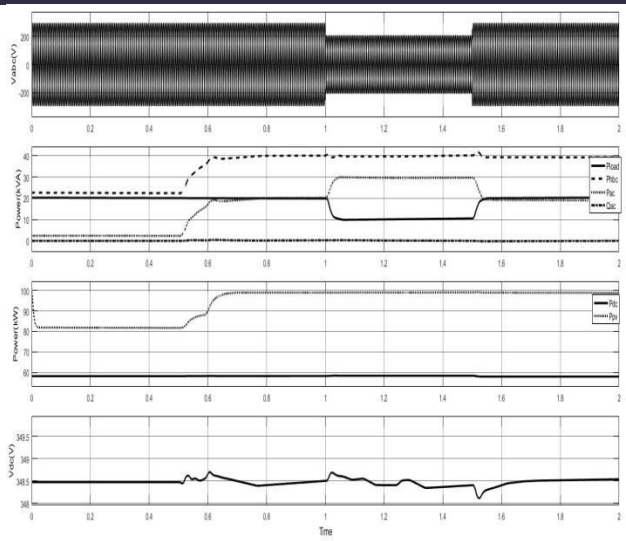

4.6 CASE 6: NICKEL-CADMIUM BATTERY PERFORMANCE

In this case the Lithium-ion battery is replaced by a Nickel-cadmium battery. From t=0 to t=0.5 seconds, MPPT is 'off'. So the PV power and PV current are not linear.

At t=0.5 seconds MPPT is turned 'on'. The MPPT by reducing the non linearity tracks maximum power from the PV panel, Hence, the PV power and PV current attains a linear value.

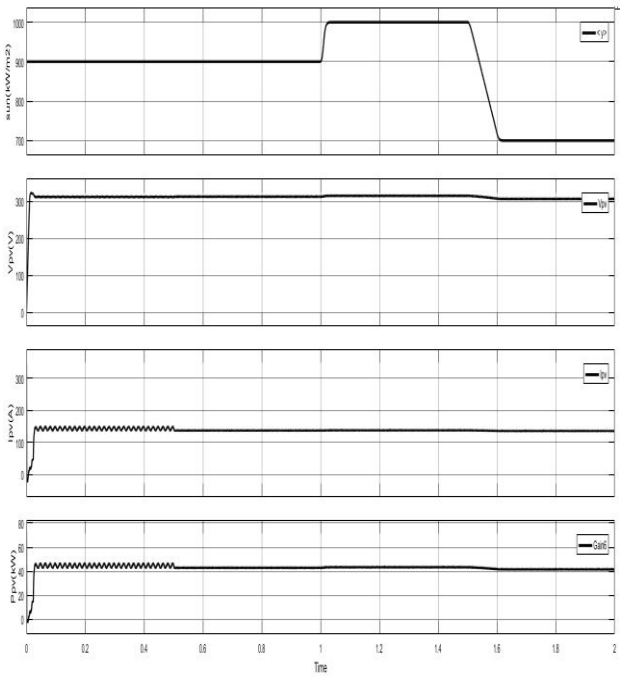

Figure 4.7 Nickel-Cadmium battery performance.

V. CONCLUSION

The PV charging station is designed by integrating PV array, ac grid, three-phase HBC, dc batteries of PHEV. Three-phase HBC is designed to replace dc/dc converter and VSC to eliminate switching losses.

The controller is designed for HBC using MPPT, PLL, and vector control schemes. One of the stochastic optimization method called Particle Swarm Optimization (PSO) is used as MPPT technique. The advantage of this method is that it can be used in large dimensional optimization problems to produce quality solutions.

Six different case studies are being conducted in MATLAB simulation to exhibit the MPPT, voltage regulation, control reactive power and power management performance of the charging station consisting of PV. The simulated outputs evaluate that the proposed control is very effective and durable to be used in PV charging station. It can also be concluded that the PHEV batteries can be charged continuously by making use of dc power from PV as well as ac grid.

REFERENCES

[1] Ahmad Tazay, Zhixin Miao, Control of a Three-Phase Hybrid Converter for a PV Charging Station , 2018,IEEE.

[2] M. Ehsani, Y. Gao, and A. Emadi, Modern electric, hybrid electric, and fuel cell vehicles: fundamentals, theory, and design. CRC press,2009.

[3] K. Sikes, T. Gross, Z. Lin, J. Sullivan, T. Cleary, and J. Ward, "Plug- in hybrid electric vehicle market introduction study: final report," Oak Ridge National Laboratory (ORNL), Tech. Rep.,2010.

[4] A.KhalighandS.Dusmez,"Comprehensivetop ologicalanalysisof con- ductive and inductive charging solutions for plug-in electric vehicles," IEEE Transactions on Vehicular Technology, vol. 61, no. 8, pp. 3475–3489,2012.

[5] T. Anegawa, "Development of quick charging system for electric vehi- cle," Tokyo Electric Power Company,2010.

[6] F. Musavi, M. Edington, W. Eberle, and W. G. Dunford, "Evaluation and efficiency comparison of front end ac-dc plug-in hybrid charger topologies," IEEE Transactions on Smart grid, vol. 3, no. 1, pp. 413– 421,2012.

[7] M. Yilmaz and P. T. Krein, "Review of battery charger topologies, charging power levels, and infrastructure for plug-in electric and hybrid vehicles," IEEE Transactions on Power Electronics, vol. 28, no. 5, pp. 2151–2169, May2013.

[8] G.Gamboa,C.Hamilton,R.Kerley,S.Elmes,A. Arias,J.Shen,andBatarseh, "Control strategy of a multi-port, grid connected, direct-dc pv charging station for plug-in electric vehicles," in Energy Conversion Congress and Exposition (ECCE), 2010 IEEE. IEEE, 2010, pp. 1173– 1177.

[9] P. Goli and W. Shireen, "Pv integrated smart charging of phevs based on dc link voltage sensing," IEEE Transactions on Smart Grid, vol. 5, no. 3, pp. 1421–1428,2014.

[10] S. Mishra, R. Adda, and A. Joshi, "Inverse watkins–johnson topology- based inverter," IEEE Transactions on Power Electronics, vol. 27, no. 3, pp. 1066–1070,2012.

[11] O. Ray and S. Mishra, "Boost-derived hybrid converter with simulta- neous dc and ac outputs," IEEE Transactions on Industry Applications, vol.50,no.2,pp.1082–1093,March2014.

[12] O. Ray, V. Dharmarajan, S. Mishra, R. Adda, and P. Enjeti, "Analysis and pwm

control of three-phase boost-derived hybrid converter," in 2014 IEEE Energy Conversion Congress and Exposition (ECCE), Sept 2014, pp.402–408.

[13] O. Ray and S. Mishra, "Integrated hybrid output converter as power router for renewable-based nanogrids," in Industrial Electronics Society, IECON 2015 - 41st Annual Conference of the IEEE, Nov 2015, pp. 001 645–001650.

[14] M. A. Elgendy, B. Zahawi, and D. J. Atkinson, "Assessment of perturb and observe mppt algorithm implementation techniques for pv pumping applications," IEEE transactions on sustainable energy, vol. 3, no. 1,pp. 21–33,2012.

[15] J. Khazaei, Z. Miao, L. Piyasinghe, and L. Fan, "Real-time digital simulation-based modeling of a single-phase single-stage pv system," ElectricPowerSystemsResearch,vol.123,pp.85–91,2015.

[16] M. Tabari and A. Yazdani, "Stability of a dc distribution system for power system integration of plug-in hybrid electric vehicles," IEEE TransactionsonSmartGrid,vol.5,no.5,pp.2564–2573,2014.

[17] O. Ray and S. Mishra, "Integrated hybrid output converter as power router for renewable-based nanogrids," in Industrial Electronics Society, IECON 2015-41st Annual Conference of the IEEE. IEEE, 2015, pp. 001 645–001650.

[18] U. Eicker, Solar technologies for buildings. John Wiley & Sons,2006.

[19] N. Femia, G. Petrone, G. Spagnuolo, and M. Vitelli, Power electronics and control techniques for maximum energy harvesting in photovoltaic systems. CRC press,2012.

[20] M. R. Patel, Wind and solar power systems: design, analysis, and operation. CRC press, 2005.

[21] O. Ellabban, J. V. Mierlo, and P. Lataire, "Comparison between different pwm control methods for different z-source inverter topologies," in Power Electronics and Applications, 2009. EPE '09. 13th European Conference on, Sept 2009, pp. 1–11.

[22] T. Esram, P. L. Chapman et al., "Comparison of photovoltaic array maximum power point tracking techniques," IEEE Transactions on Energy Conversion EC, vol. 22, no. 2, p. 439, 2007.

[23] C. Dorofte, U. Borup, and F. Blaabjerg, "A combined two-method mppt control scheme for grid-connected photovoltaic systems," in Power electronics and applications, 2005 European conference on. IEEE,2005, pp. 10–pp.

[24] "Ieee standard for interconnecting distributed resources with electric power systems," IEEE Std 1547-2003, pp. 1–28, July 2003.

[25] D. Dong, B. Wen, D. Boroyevich, P. Mattavelli, and Y. Xue, "Analysis of phase-locked loop low-frequency stability in three-phase grid-connected power converters considering impedance interactions," IEEE Transactions on Industrial Electronics, vol. 62, no. 1, pp. 310–321, Jan 2015.

[26] A. Yazdani and R. Iravani, Voltage-sourced converters in power systems: modeling, control, and applications. John Wiley & Sons, 2010.

[27] A. Tazay, Z. Miao, and L. Fan, "Blackstart of an induction motor in an autonomous microgrid," in 2015 IEEE Power Energy Society General Meeting, July 2015, pp. 1–5.

[28] F. Fr¨ohr and F. Orttenburger, Introduction to electronic control engineering. Heyden, 1982.

[29] Y. Hu, S. Yurkovich, Y. Guezennec, and B. Yurkovich, "A technique for dynamic battery model identification in automotive applications using linear parameter varying structures," Control Engineering Practice,vol. 17, no. 10, pp. 1190–1201, 2009.

[30] C. C. Grant, US National Electric Vehicle Safety Standards Summit: Summary Report. Fire Protection Research Foundation, 2010.

[31] "Electric vehicle and plug-in hybrid electric vehicle conductive charge coupler," SAE J1772, Jan 2010.

[32] P. Fan, B. Sainbayar, and S. Ren, "Operation analysis of fast charging stations with energy demand control of electric vehicles," IEEE Transactions on Smart Grid, vol. 6, no. 4, pp. 1819–1826, July 2015.

[33] D. Linden, "Handbook of batteries and fuel cells," New York, McGraw-Hill Book Co., 1984, 1075 p. No individual items are abstracted in this volume., vol. 1, 1984.

[34] M. S. Rahman, M. Hossain, and J. Lu, "Coordinated control of threephase ac and dc type ev–esss for efficient hybrid microgrid operations,"Energy Conversion and Management, vol. 122, pp. 488–503, 2016.

[35] J. Y. Yong, V. K. Ramachandaramurthy, K. M. Tan, and J. Selvaraj, "Experimental validation of a three-phase off-board electric vehicle charger with new power grid voltage control," IEEE Transactions on Smart Grid, 2016.

[36] N. Leaf, "2011 leaf owner's manual revised," 2011. [Online]. Available: http://www.nissan-techinfo.com/refgh0v/og/leaf/2011-nissan-leaf.pdf

[37] G.Motors," 2016 chev rolet volt battery system,"2016[Online].Available: https://media.gm.com/content/dam/Media/microsites/product/Volt2016/doc/VOLT_BATTERY.pdf

[38] "Ieee standard for performance criteria and test methods for plug-in (portable) multiservice (multiport) surge-protective devices for equipment connected to a 120 v/240 v single phase power service and metallic conductive communication line(s)," IEEE Std C62.50-2012, pp. 1–63,Sept 2012.